

Dielectric Relaxation Profiles in a Theory of Interfacial Polarization Developed for Concentrated Disperse Systems of Spherical Particles

Tetsuya HANAI, Yasuo KITA, and Naokazu KOIZUMI*

Received October 2, 1980

Numerical computation was carried out to obtain dielectric relaxation profiles in a theory of interfacial polarization, which was proposed by Hanai [*Kolloid Z.*, **171**, 23 (1960)], applicable to concentrated disperse systems of spherical particles. The relaxation profiles computed for the case of W/O emulsions in higher concentrations are found to have features different from skewed arcs as well as from circular arcs, being simulated satisfactorily with deformed circular arcs proposed by Williams and Watts. Further consideration reveals that dielectric relaxation profiles in various types other than a single relaxation system are predictable from this theory without an assumption of the distribution of relaxation times.

KEY WORDS: Dielectric relaxation / Interfacial polarization / Disperse system / Emulsion / Circular arc / Skewed arc / Single relaxation / Relative permittivity / Electric conductivity / Williams-Watts' equation /

I INTRODUCTION

It is known that heterogeneous systems of spherical particles dispersed in a continuous phase show dielectric relaxations due to interfacial polarization. The dielectric relaxations were discussed by many workers¹⁻⁴⁾ qualitatively in the light of Wagner's theory.⁵⁾ Since closer consideration revealed that Wagner's theory was in agreement with experimental results only at lower concentrations of the disperse phase, Hanai^{6,7)} proposed a theory which is expected to be applicable to higher concentrations as well as to lower concentrations.

According to our dielectric study of water-in-oil (W/O) emulsions,^{8,9)} remarkable dielectric relaxations were observed in accordance with Hanai's theory, and the limiting relative permittivities at high frequencies showed excellent agreements with the theory. In our previous observation on the dielectric relaxations of W/O emulsions,⁹⁾ the limiting relative permittivities at low frequencies were also in good agreements with the theory as far as the W/O emulsions were prepared by minimal use of emulsifiers.

Since the expression of this theory is of a very complicated function form with respect to complex variables, it was impossible to calculate the relative permittivities and the electric conductivities predictable from the theory at arbitrary frequencies.

* 花井哲也, 喜多保夫, 小泉直一: Laboratory of Dielectrics, Institute for Chemical Research, Kyoto University, Uji, Kyoto.

Hence the profiles of dielectric relaxations were not elucidated in this theory.

Recently some attempts have been made to calculate the relative permittivities and the electric conductivities deduced from the theory by the use of computers. Clause¹⁰⁻¹⁴⁾ performed computer analyses of this theoretical formula for the purpose of discussing his data on emulsions and microemulsions. Further Clause and the collaborators¹⁵⁾ showed a routine-program for FORTRAN so as to obtain the roots of this theoretical equation. According to their algorithm, it is not possible to select a proper and unique root while computing. Physical considerations such as the signs and relative magnitudes of real and imaginary parts of the roots and continuity with respect of frequency are required to obtain such a selection.

Hanai and Koizumi¹⁶⁾ established algorithm in which improper roots were ruled out by mathematical inspection and only the physically significant roots were adopted. By using this algorithm one can obtain realistic solutions of the theoretical equation at arbitrary frequencies, being able to discuss the frequency dependence of the relative permittivities and electric conductivities derived from the theory.

In the present study, relative permittivities and electric conductivities for Hanai's theory⁶⁾ are calculated by means of the computation mentioned above, and the related profiles of dielectric relaxations are discussed for some typical cases of spherical disperse systems. Some comparisons are made between this theory and others.

II GLOSSARY OF SYMBOLS

| | |
|--------------|---|
| ϵ_a | relative permittivity (dielectric constant) of the continuous medium. |
| κ_a | electric conductivity of the continuous medium, S cm ⁻¹ . |
| ϵ_i | relative permittivity of the disperse phase. |
| κ_i | electric conductivity of the disperse phase, S cm ⁻¹ . |
| ϵ | relative permittivity of the disperse system. |
| κ | electric conductivity of the disperse system, S cm ⁻¹ . |

ϵ_a^* , ϵ_i^* , and ϵ^* are complex relative permittivity of the continuous medium, the disperse phase and the disperse system respectively, being given by

$$\epsilon_a^* = \epsilon_a - j \frac{\kappa_a}{2\pi f \epsilon_v} \quad (1)$$

$$\epsilon_i^* = \epsilon_i - j \frac{\kappa_i}{2\pi f \epsilon_v} \quad (2)$$

and
$$\epsilon^* = \epsilon - j \frac{\kappa}{2\pi f \epsilon_v} \quad (3)$$

f measuring frequency, Hz.

j unit imaginary, $\sqrt{-1}$.

ϵ_v permittivity of vacuum given by

$$\epsilon_v = \frac{1}{4\pi \cdot 9 \cdot 10^{11}} = 8.8541853 \times 10^{-14} \text{F cm}^{-1}. \quad (4)$$

- Φ volume fraction of the disperse phase.
 ϵ_l limiting relative permittivity at low frequencies.
 ϵ_h limiting relative permittivity at high frequencies.
 κ_l limiting conductivity at low frequencies, S cm⁻¹.
 κ_h limiting conductivity at high frequencies, S cm⁻¹.
 f_0 relaxation frequency characteristic of the dielectric relaxation, Hz.
 $\Delta\epsilon$ magnitude or intensity of the dielectric relaxation, being given by $\Delta\epsilon = \epsilon_l - \epsilon_h$.
 $\Delta\epsilon''$ imaginary part of the complex relative permittivity or loss factor associated with the dielectric relaxation, being expressed as

$$\Delta\epsilon'' = \frac{\kappa - \kappa_l}{2\pi f \epsilon_v} \quad (5)$$

- $\Delta\epsilon''_{\max}$ maximum value of the dielectric loss factor $\Delta\epsilon''$ against frequency.
 $\Delta\kappa''$ imaginary part of the complex electric conductivity, being expressed as

$$\Delta\kappa'' = 2\pi f \epsilon_v (\epsilon - \epsilon_h) \quad (6)$$

E' and E'' are normalized real part and imaginary part or loss factor of relative permittivity, being expressed as

$$E' = \frac{\epsilon - \epsilon_h}{\epsilon_l - \epsilon_h}, \quad (7)$$

and

$$E'' = \frac{\Delta\epsilon''}{\epsilon_l - \epsilon_h} = \frac{\kappa - \kappa_l}{2\pi f \epsilon_v (\epsilon_l - \epsilon_h)} \quad (8)$$

K' and K'' are normalized real part and imaginary part of the complex conductivity, being expressed as

$$K' = \frac{\kappa - \kappa_l}{\kappa_h - \kappa_l}, \quad (9)$$

and

$$K'' = \frac{\Delta\kappa''}{\kappa_h - \kappa_l} = 2\pi f \epsilon_v \frac{\epsilon - \epsilon_h}{\kappa_h - \kappa_l} \quad (10)$$

β and α distribution parameters of relaxation times.

III THEORETICAL FORMULAS FOR INTERFACIAL POLARIZATION

According to Wagner's theory⁵⁾ of interfacial polarization, the complex relative permittivity ϵ^* for a dilute disperse system of spherical particles is given by

$$\epsilon^* = \epsilon_a^* \frac{2(1 - \Phi)\epsilon_a^* + (1 + 2\Phi)\epsilon_i^*}{(2 + \Phi)\epsilon_a^* + (1 - \Phi)\epsilon_i^*} \quad (11)$$

Frequency dependence of the relative permittivities ϵ and the conductivities κ derived by Eq. (11) is characterized with a single relaxation type, and complex

plane plots of both the complex relative permittivities and the complex conductivities are represented by semicircles.³⁾

For a concentrated disperse system of spherical particles, Hanai^{6,7)} proposed the following equation for a complex relative permittivity of the system.

$$\frac{\epsilon^* - \epsilon_i^*}{\epsilon_a^* - \epsilon_i^*} \left(\frac{\epsilon_a^*}{\epsilon^*} \right)^{1/3} = 1 - \Phi. \quad (12)$$

In a previous paper¹⁶⁾ the procedure was proposed by which to solve Eq. (12) and choose sets of ϵ and κ of physical significance. The present paper deals mainly with the dielectric relaxation profiles derived from Eq. (12).

IV RELAXATION PROFILE RELATED TO W/O EMULSIONS

In Fig. 1 is shown the frequency dependence of relative permittivity ϵ , electric conductivity κ and loss factor $\Delta\epsilon''$ calculated from Hanai's Eq. (12) and Eq. (5) for a set of phase parameters relating to W/O emulsions: $\epsilon_a=2.1$, $\kappa_a=6.55 \times 10^{-5} \mu\text{S cm}^{-1}$, $\epsilon_i=77.5$, $\kappa_i=24.5 \mu\text{S cm}^{-1}$, $\Phi=0.98$. The data shown in Fig. 1 are plotted on complex planes of complex relative permittivity and complex conductivity, and are shown in Figs. 2 and 3 where $\Delta\kappa''$ is calculated with Eq. (6). For reference, dielectric behavior of a single relaxation system is shown with dashed curves in the Figures. The curves by Eq. (12) in Figs. 1, 2 and 3 show the shape different distinctly from semicircles and circular arcs.

Characteristic profiles of the dielectric relaxation can be exhibited comprehensively in terms of normalized permittivity E' (Eq. (7)), normalized loss factor E'' (Eq. (8)),

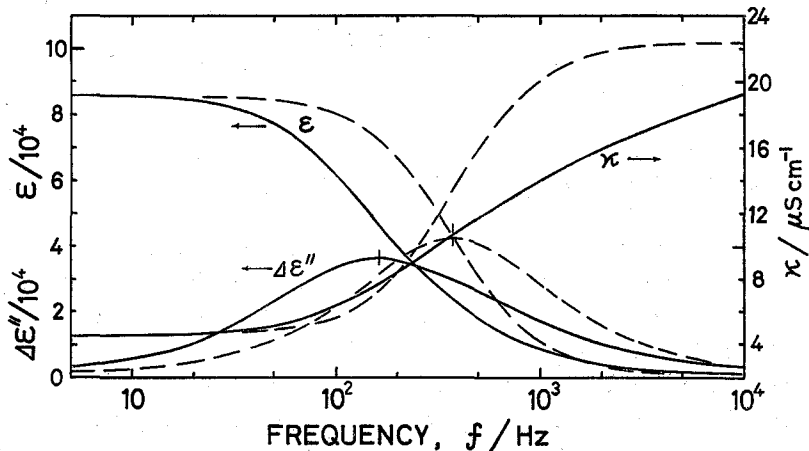


Fig. 1. Frequency dependence of the relative permittivity ϵ , the electric conductivity κ and the loss factor $\Delta\epsilon'' = (\kappa - \kappa_i) / (2\pi f \epsilon_0)$ calculated from Hanai's Eq. (12). The phase parameters used: $\epsilon_a=2.1$, $\kappa_a=6.55 \times 10^{-5} \mu\text{S cm}^{-1}$, $\epsilon_i=77.5$, $\kappa_i=24.5 \mu\text{S cm}^{-1}$ and $\Phi=0.98$. Dashed curves are single relaxation profiles with the same values of ϵ_i , ϵ_a , κ_i and κ_a as calculated from Eq. (12).

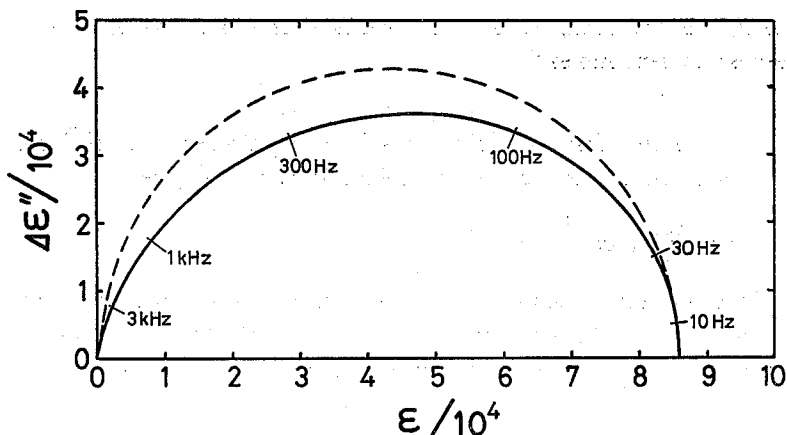


Fig. 2. Complex plane plots of ϵ and $\Delta\epsilon''$ with the same data as shown in Fig. 1.

The solid curve is given by Hanai's Eq. (12), the dashed curve (semicircle) by a single relaxation system. Numbers along the curve are the frequency.

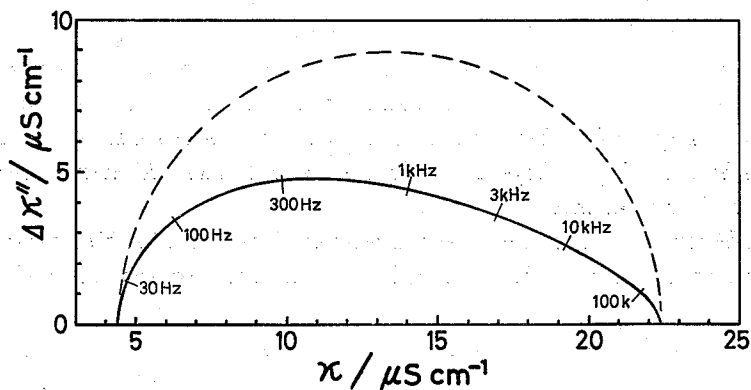


Fig. 3. Complex plane plots of κ and $\Delta\kappa''=2\pi f\epsilon_0(\epsilon-\epsilon_h)$ with the same data as shown in Fig. 1.

The solid curve is given by Hanai's Eq. (12), the dashed curve (semicircle) by a single relaxation system. Numbers along the solid curve are the frequency.

and normalized real part K' and imaginary part K'' of the complex conductivity (Eqs. (9) and (10)). Figures 4 and 5 show the change in E'' with E' and the change in K'' with K' calculated from Eq. (12) at volume fractions $\phi=0.4, 0.6, 0.8$ and 0.98 with the same values of $\epsilon_a, \kappa_a, \epsilon_i$ and κ_i .

The relaxation profiles represented on the $E'-E''$ plane (Fig. 4) and on the $K'-K''$ plane (Fig. 5) show variety of types with the increase in the volume fraction ϕ . At lower concentrations ($\phi \leq 0.4$) the profiles seem to be close to semicircles, the characteristics being the same as those given by Wagner's Eq. (11). At medium concentrations ($\phi=0.4-0.6$), the profiles may be approximated with circular arcs which are shown later by Eq. (14). At higher concentrations ($\phi \geq 0.6$) the profiles are seen to show remarkable deviation from circular arcs, and are simulated with Williams-

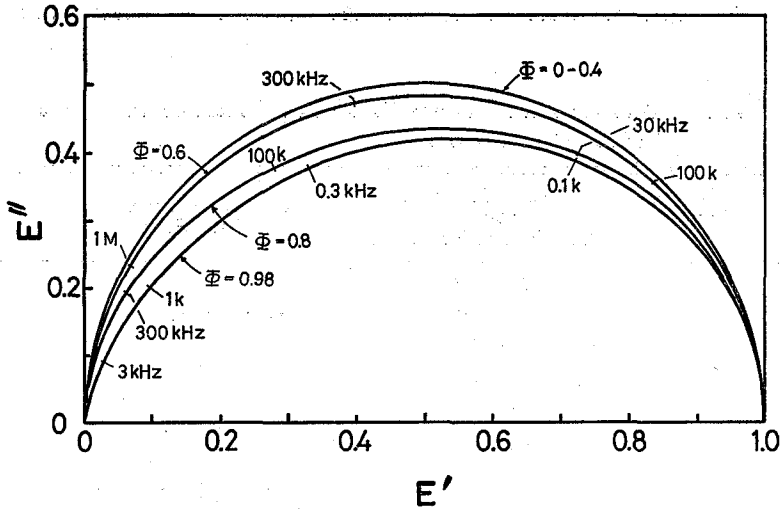


Fig. 4. Complex plane plots of the normalized permittivity E' and the normalized loss factor E'' calculated from Hanai's Eq. (12) at different concentrations ϕ .

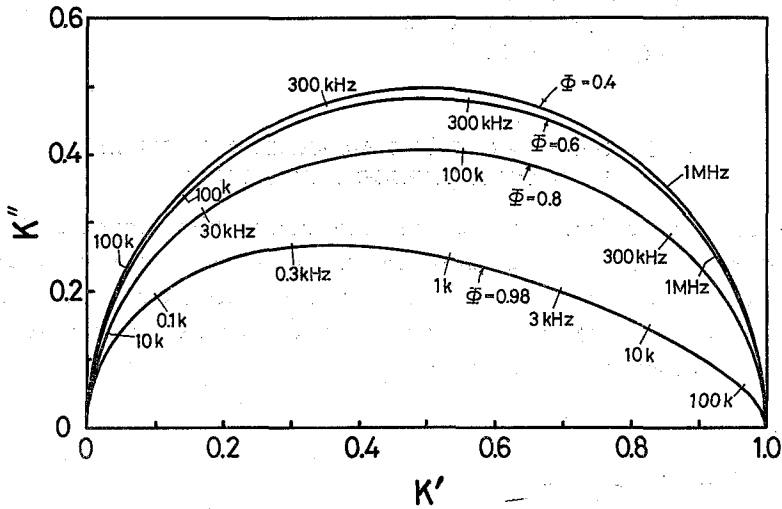


Fig. 5. Complex plane plots of the normalized real part K' and the imaginary part K'' of the complex conductivity with the same data as shown in Fig. 4.

Watts' formulas which will be discussed in the succeeding section. The characteristics of the complex plane plots of Hanai's Eq. (12) are summarized in Table I.

In the case of an O/W emulsion with a set of phase parameters $\epsilon_a=77.5$, $\kappa_a=24.5 \mu\text{S cm}^{-1}$, $\epsilon_i=2.1$, $\kappa_i=6.55 \times 10^{-5} \mu\text{S cm}^{-1}$, and $\phi=0.8$, Eq. (12) gives the value $\epsilon_1=9.800$ and $\epsilon_2=9.637$. We have thus $\Delta\epsilon=\epsilon_1-\epsilon_2=0.163$, which means that the dielectric relaxation for this O/W emulsion is too small to be observed. In accordance with this prediction by Eq. (12), Hanai, Koizumi, and Gotoh¹⁷⁾ observed no dielectric relaxation due to the interfacial polarization in O/W emulsions. The relaxation

profiles for O/W emulsion need not be discussed from such an experimental point of view.

Table I. Characteristics of Complex Plane Plots of Hanai's Equation (12) at Different Concentrations

| Volume Fraction ϕ | The α -Value when Simulated by Circular Arc Eq. (14) | Features of Complex Plane Plots |
|------------------------|---|---|
| 0.1 | 0.000016 | Nearly semicircles. |
| 0.2 | 0.000032 | |
| 0.3 | 0.0022 | |
| 0.4 | 0.0051 | |
| 0.5 | 0.011 | Nearly circular arc. |
| 0.6 | 0.024 | |
| 0.7 | 0.055 | |
| 0.8 | 0.086 | Remarkable deviation from circular arc. Excellent simulation by a Williams-Watts type. |
| 0.9 | 0.123 | |
| 0.98 | 0.115 | |

Phase parameters used for calculating Eq. (12):

$$\epsilon_a = 2.1, \quad \kappa_a = 6.55 \times 10^{-5} \mu\text{S cm}^{-1},$$

$$\epsilon_t = 77.5, \quad \kappa_t = 24.5 \mu\text{S cm}^{-1}.$$

V COMPARISONS OF THE RELAXATION PROFILES WITH SOME EMPIRICAL FORMULAS

As readily seen in Figs. 1 and 2, the relaxation profiles derived from Eq. (12) show the deviation from a single relaxation system and semicircles which are predictable from Wagner's Eq. (11). In this Section, these characteristic profiles of Eq. (12) are compared with the following empirical formulas which have been proposed so far to express relaxation types of dielectrics.

i) Semicircular Arc Rule

$$E' - jE'' = \frac{1}{1 + jf/f_0} \quad (13)$$

This formula, called a single relaxation type, gives a semicircle on complex planes of $E' - E''$.

ii) Circular Arc Rule¹⁸⁾

$$E' - jE'' = \frac{1}{1 + (jf/f_0)^\beta} = \frac{1}{1 + (jf/f_0)^{1-\alpha}}, \quad (14)$$

$$0 < \beta \leq 1, \quad 0 \leq \alpha < 1.$$

where β and α are distribution parameters of relaxation times.

Numerical tables of E' and E'' with respective β 's for this Eq. (14) were reported by Koizumi, Hanai, and Ikada.¹⁹⁾

iii) Skewed Arc Rule²⁰⁾

$$E' - jE'' = \frac{1}{(1 + jf/f_0)^\beta} \quad 0 < \beta \leq 1 \quad (15)$$

Numerical tables of E' and E'' with respective β 's for this Eq. (15) are readily prepared because of simple function forms of these E' and E'' .

iv) Deformed Arc Rule Proposed by Williams and Watts^{21,22)}

$$E' - jE'' = \int_0^\infty [2\pi f_0 \beta (2\pi f_0 t)^{-(1-\beta)} \cdot \exp\{-(2\pi f_0 t)^\beta\}] \exp(-j2\pi ft) dt. \quad (16)$$

Numerical tables of these E' and E'' with respective β 's were presented by Koizumi and Kita.²³⁾

The data of Eq. (12) shown in Figs. 1 and 2 are transformed to E' and E'' , being shown in Figs. 6, 7 and 8. An analytical formula of loss maximum frequency is not derived yet in Hanai's theory given by Eq. (12). According to numerical inspection for Eq. (12), the loss maximum frequency was found to be distinctly different from the frequency giving the half value of the dielectric relaxation intensity. From an experimental point of view, it is difficult to determine with precision the loss maximum frequency as against the half-value frequency for the magnitude of the dielectric relaxation. Only for Eq. (12) of Hanai's theory, therefore, the symbol f_0 is used as the relaxation frequency at which the relative permittivity shows a half value of the magnitude of the dielectric relaxation.

By the searching in the numerical tables cited above, adequate values of respective β 's can be found so that Eqs. (14), (15) and (16) may take the same values as Eq. (12) with regard to the maxima of the normalized loss factor E'' against frequency. The

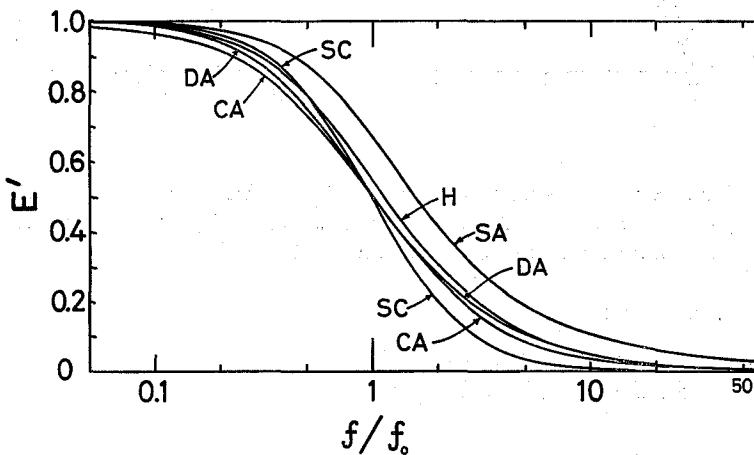


Fig. 6. Dependence of the normalized permittivity E' upon the normalized frequency f/f_0 . The curve H, Hanai's Eq. (12); SC, Semicircular arc Eq. (13); CA, Circular arc Eq. (14) with $\beta=0.89$; SA, Skewed arc Eq. (15) with $\beta=0.69$; DA, Deformed arc Eq. (16) with $\beta=0.81$.

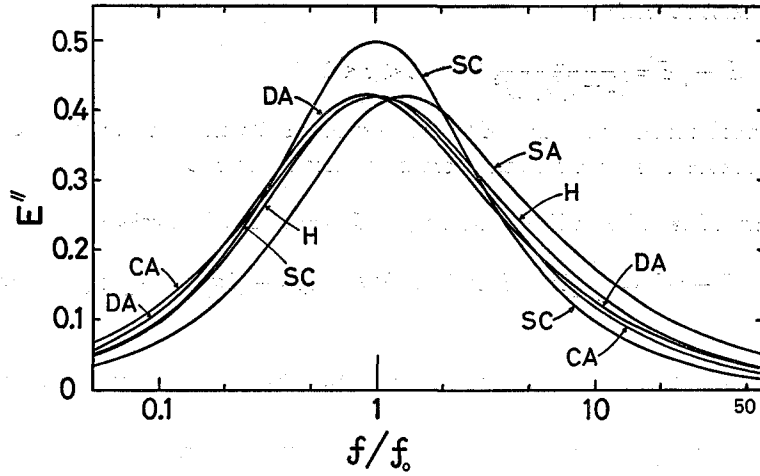


Fig. 7. Dependence of the normalized loss factor E'' upon the normalized frequency f/f_0 . Abbreviated names of the curves are the same as those in Fig. 6.

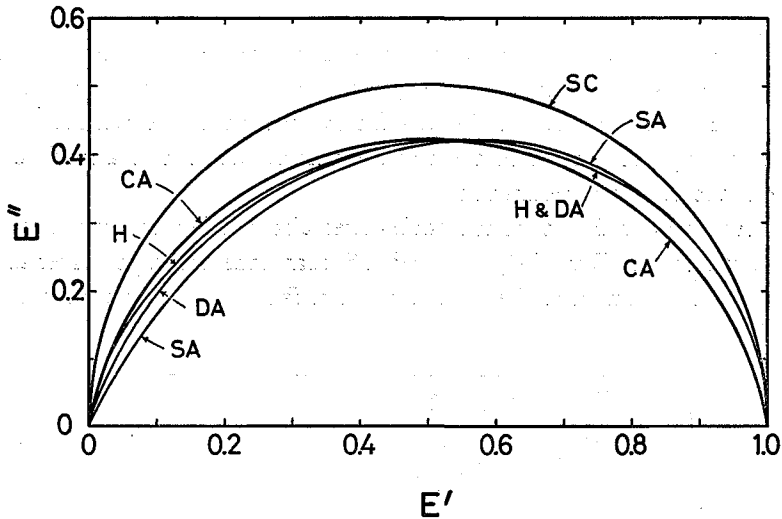


Fig. 8. Complex plane plots of E' and E'' derived from different formulas: Eqs. (12), (13), (14), (15) and (16). The same data as shown in Fig. 6 and 7. Abbreviated names of the curves are the same as those in Fig. 6.

values thus estimated was

$$\beta=0.89 \quad \text{for the circular arc Eq. (14),}$$

$$\beta=0.69 \quad \text{for the skewed arc Eq. (15),}$$

and

$$\beta=0.81 \quad \text{for the deformed arc Eq. (16).}$$

The frequency dependence of E' and E'' and the relation between E' and E'' are calculated from Eqs. (14), (15) and (16) with respective values of β just determined, being shown in Figs. 6, 7 and 8 together with the curves by the semicircle Eq. (13).

In Figs. 6 and 7 the curves of Eq. (13) for semicircles are seen to show the most abrupt change with frequency, other curves showing a little difference from one another. In Fig. 8 marked differences are seen among the curves. The semicircle of Eq. (13) and the circular arc of Eq. (14) show remarkable deviations from the curve of Hanai's Eq. (12) over the whole range of frequency. The skewed arc of Eq. (15) is very close to the curve of Eq. (12) at lower frequencies (the right half of Fig. 8), and shows marked deviation from the curve of Eq. (12) at higher frequencies (the left half of Fig. 8).

The deformed arc of Eq. (16) is very close to the curve of Eq. (12) over the whole range of frequency with little deviation in the left half of Fig. 8. On the other hand, Eq. (16) with β -values close to unity approaches the circular arc Eq. (14) which represents the feature of Eq. (12) in lower concentrations as shown in Fig. 4 and Table I. It is concluded therefore that the deformed arc rule proposed by Williams and Watts simulates fairly well the relaxation profiles of Hanai's Eq. (12) over the whole range of concentration.

VI EVALUATION OF THE RELAXATION INTENSITY FROM THE DIELECTRIC LOSS DATA

Kita and Koizumi²⁴⁾ proposed a method to evaluate the relaxation intensity $\Delta\epsilon$ by the use of $\Delta\epsilon''_{\max}$ and the two frequencies designated by a certain value of $\Delta\epsilon''/\Delta\epsilon''_{\max}$, where $\Delta\epsilon''_{\max}$ is the loss maximum. This method was applied to the data shown in Fig. 1 for respective values $\Delta\epsilon''/\Delta\epsilon''_{\max}=1/2, 2/3$ and $3/4$. The results obtained are summarized in Table II together with the value of $\Delta\epsilon$ directly calculated from Eq. (12). As readily seen in the Table, the values of $\Delta\epsilon$ deduced from the deformed arc by Williams-Watts are closest to that calculated from Eq. (12), this result being in accord with the conclusion in Section V and Fig. 8.

Table II. Comparison of the Relaxation Intensity $\Delta\epsilon$ Evaluated from Dielectric Loss Data

| $\frac{\Delta\epsilon''}{\Delta\epsilon''_{\max}}$ | Relaxation Intensity $\Delta\epsilon$ Evaluated for the Relaxation Type of | | | |
|--|--|--------------------------------|-----------------------------------|---|
| | Circular Arc by Cole-Cole | Skewed Arc by Davidson-Cole | Deformed Arc by Williams-Watts | Compromise between Davidson-Cole and Williams-Watts |
| 1/2 | 87500 | 89800 | 87300 | 87500 |
| 2/3 | 88200 | 91800 | 87700 | — |
| 3/4 | 87800 | 92000 | 87200 | — |
| mean | 87800 | 91200 | 87400 | — |

$$\Delta\epsilon = \epsilon_l - \epsilon_h \text{ by Eq. (12) } = 85800$$

**VII RELAXATION PROFILES OF HANAI'S EQUATION
IN SOME PARTICULAR CASES**

As a particular example, frequency dependence of ϵ , κ and $\Delta\epsilon''$ were computed from Hanai's Eq. (12) with a set of phase parameters of the followings:

$$\begin{aligned} \epsilon_a &= 2, & \kappa_a &= 30 \mu\text{S cm}^{-1} \\ \epsilon_i &= 80, & \kappa_i &= 1 \mu\text{S cm}^{-1}, & \Phi &= 0.8. \end{aligned}$$

The results of the calculations are shown in Figs. 9, 10 and 11 together with the dashed curves expressing a single relaxation type. Evidently the curves derived from Eq. (12) show very remarkable deviation from those in a single relaxation type. In particular the dielectric relaxation profile as seen in Figs. 9 and 10 looks like the composite behavior of two kinds of a single relaxation mechanism. The similar pattern

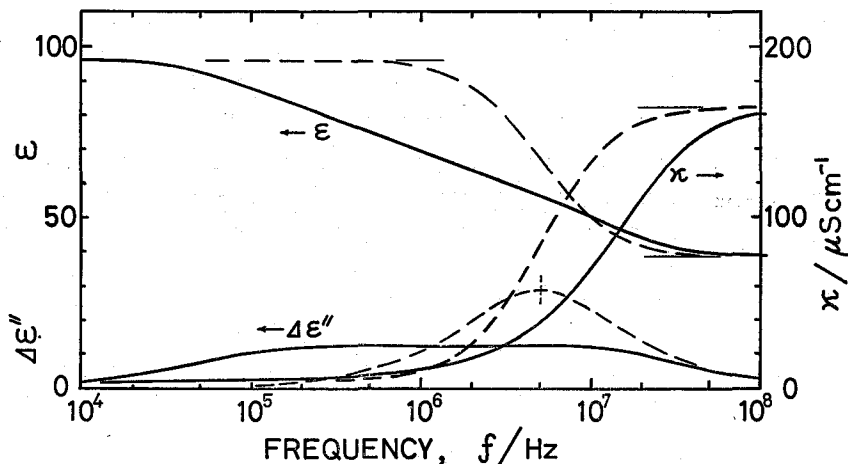


Fig. 9. Frequency dependence of the relative permittivity ϵ , the electric conductivity κ and the loss factor $\Delta\epsilon''$ calculated from Hanai's Eq. (12).

The phase parameters used: $\epsilon_a=2$, $\kappa_a=30 \mu\text{S cm}^{-1}$, $\epsilon_i=80$, $\kappa_i=1 \mu\text{S cm}^{-1}$ and $\Phi=0.8$. Dashed curves are single relaxation profiles with the same values of ϵ_i , ϵ_h , κ_i and κ_h as calculated from Eq. (12).

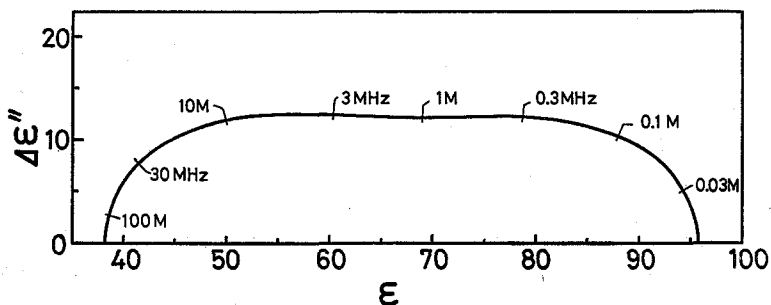


Fig. 10. Complex plane plots of ϵ and $\Delta\epsilon''$ with the same data as shown in Fig. 9.

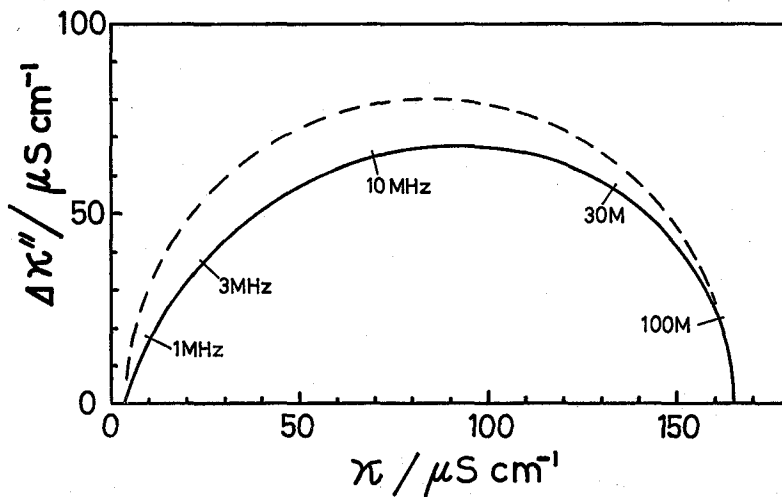


Fig. 11. Complex plane plots of κ and $\Delta\kappa''$ with the same data as shown in Fig. 9.

The solid curve is given by Hanai's Eq. (12), the dashed curve (semicircle) by a single relaxation system.

was observed by Ballario, Bonincontro, and Cametti,²⁵⁾ for polystyrene aqueous suspensions with low ionic conductivity.

Another peculiar example is dielectric relaxation profiles computed from Hanai's Eq. (12) with a set of phase parameters of the followings:

$$\begin{aligned} \epsilon_a &= 80, & \kappa_a &= 1 \mu\text{S cm}^{-1} \\ \epsilon_i &= 2, & \kappa_i &= 30 \mu\text{S cm}^{-1}, & \Phi &= 0.8. \end{aligned}$$

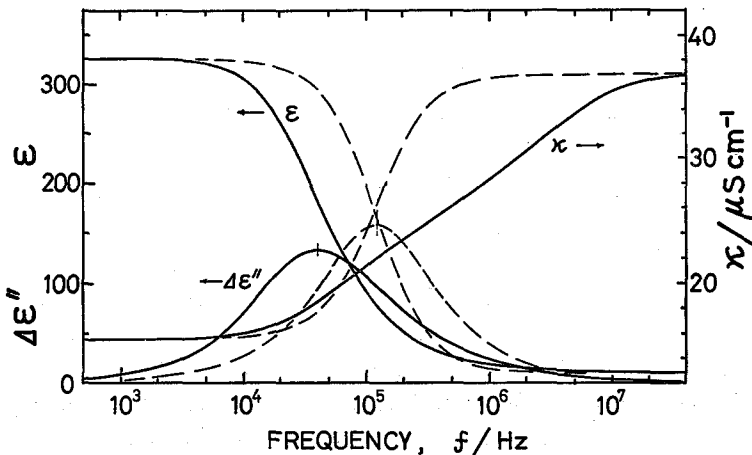


Fig. 12. Frequency dependence of the relative permittivity ϵ , the electric conductivity κ and the loss factor $\Delta\epsilon''$ calculated from Hanai's Eq. (12).

The phase parameters used: $\epsilon_a=80$, $\kappa_a=1 \mu\text{S cm}^{-1}$, $\epsilon_i=2$, $\kappa_i=30 \mu\text{S cm}^{-1}$ and $\Phi=0.8$. Dashed curves are single relaxation profiles with the same values of ϵ_i , ϵ_h , κ_i and κ_h as calculated from Eq. (12).

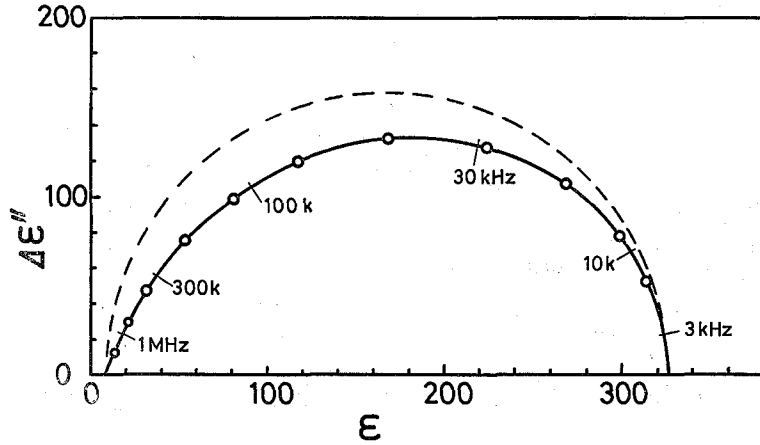


Fig. 13. Complex plane plots of ϵ and $\Delta\epsilon''$ with the same data as shown in Fig. 12.

The solid curve is given by Hanai's Eq. (12), the dashed curve (semicircle) by a single relaxation system. Open circles \circ represent the values calculated from the deformed arc Eq. (16) with $\beta=0.81$. The deformed arc Eq. (16) is seen to simulate satisfactorily the profile of Hanai's Eq. (12) in view of this finding that the open circles are just on the solid curve.

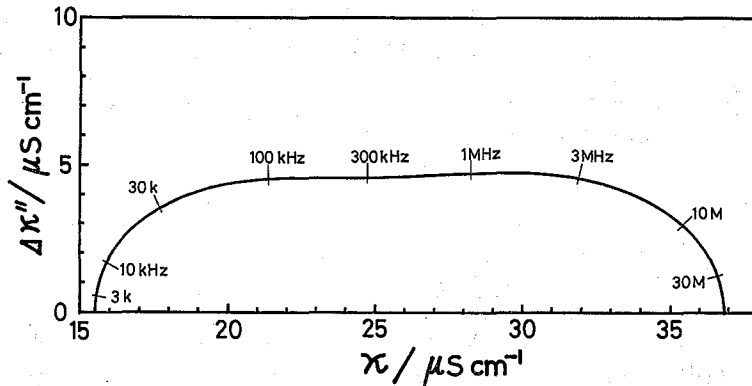


Fig. 14. Complex plane plots of κ and $\Delta\kappa''$ with the same data as shown in Fig. 12.

The results are shown in Figs. 12, 13 and 14 together with the dashed curves expressing a single relaxation type. In this instance the shape of the curve on the complex plane plots of ϵ^* shown in Fig. 13 seems to be a kind of the deformed arc type.

After the searching in the numerical tables,²³⁾ an adequate value $\beta=0.81$ for the deformed arc Eq. (16) was found to simulate the curve derived from Eq. (12). The values calculated from Eq. (16) are shown with hollow circles in Fig. 13. It is concluded that the deformed arc rule simulates very satisfactorily the relaxation profiles of Hanai's Eq. (12).

As regards relaxation types of dielectrics, complex permittivity plots showing deviation from semicircles are sometimes interpreted with the distribution of relaxation

times. Nevertheless different types of complex permittivity plots can be derived from Hanai's Eq. (12) without any assumption of distribution of relaxation times.

REFERENCES

- (1) L. K. H. van Beek, Dielectric Behaviour of Heterogeneous Systems, in "Progress in Dielectrics," Vol. 7, ed. by J. B. Birks, Heywood Books, London, 1967, pp. 69-114.
- (2) S. S. Dukhin, Dielectric Properties of Disperse Systems, in "Surface and Colloid Science," Vol. 3, ed. by Egon Matijević, Wiley-Interscience, New York and London, 1971, pp. 83-165.
- (3) T. Hanai, Electrical Properties of Emulsions, in "Emulsion Science," Chapter 5, ed. by P. Sherman, Academic Press, London and New York, 1968, pp. 353-478.
- (4) H. P. Schwan, Electrical Properties of Tissue and Cell Suspensions, in "Advances in Biological and Medical Physics," Vol. V, ed. by J. H. Lawrence and C. A. Tobias, Academic Press, New York, 1957, pp. 147-209.
- (5) K. W. Wagner, *Arch. Electrotech.*, **2**, 371 (1914).
- (6) T. Hanai, *Kolloid Z.*, **171**, 23 (1960).
- (7) T. Hanai, *Kolloid Z.*, **175**, 61 (1961).
- (8) T. Hanai, *Kolloid Z.*, **177**, 57 (1961).
- (9) T. Hanai and N. Koizumi, *Bull. Inst. Chem. Res., Kyoto Univ.*, **53**, 153 (1975).
- (10) M. Clause, Thèse de Doctorat ès sciences physiques, The University of Pau, (1971).
- (11) M. Clause, *Comptes rendus*, **274B**, 649 (1972).
- (12) M. Clause, *Comptes rendus*, **274B**, 887 (1972).
- (13) M. Clause, *Comptes rendus*, **275B**, 427 (1972).
- (14) J. Peyrelasse, C. Boned, P. Xans, and M. Clause, "Emulsions, Latexes, and Dispersions," ed. by Paul Becher and Marvin N. Yudenfreund, Marcel Dekker Inc., New York and Basel, 1978, pp. 221-236.
- (15) M. Clause and R. Royer, "Colloid and Interface Science," Vol. II, ed. by Milton Kerker, Academic Press Inc., New York, 1976, pp. 217-232.
- (16) T. Hanai and N. Koizumi, *Bull. Inst. Chem. Res., Kyoto Univ.*, **54**, 248 (1976).
- (17) T. Hanai, N. Koizumi, and R. Gotoh, *Kolloid Z.*, **167**, 41 (1959).
- (18) K. S. Cole and R. H. Cole, *J. Chem. Phys.*, **9**, 341 (1941).
- (19) N. Koizumi, T. Hanai, and E. Ikada, *Bull. Inst. Chem. Res., Kyoto Univ.*, **49**, 268 (1971).
- (20) D. W. Davidson and R. H. Cole, *J. Chem. Phys.*, **18**, 1417 (1950).
- (21) G. Williams and D. C. Watts, *Trans. Faraday Soc.*, **66**, 80 (1970).
- (22) G. Williams, D. C. Watts, S. B. Dev, and A. M. North, *Trans. Faraday Soc.*, **67**, 1323 (1971).
- (23) N. Koizumi and Y. Kita, *Bull. Inst. Chem. Res., Kyoto Univ.*, **56**, 300 (1978).
- (24) Y. Kita and N. Koizumi, *Adv. Mol. Relax. Inter. Proc.*, **15**, 261 (1979).
- (25) C. Ballario, A. Bonincontro, and C. Cametti, *J. Colloid Interface Sci.*, **54**, 415 (1976).